

Discovery of New Metastable Patterns in Diblock Copolymers

Kai Jiang^{1,2}, Chu Wang¹, Yunqing Huang² and Pingwen Zhang^{1,*}

¹ LMAM and School of Mathematical Sciences, Peking University, Beijing 100871, P.R. China.

² Hunan Key Laboratory for Computation and Simulation in Science and Engineering, Xiangtan University, Xiangtan 411105, P.R. China.

Received 15 August 2011; Accepted (in revised version) 11 October 2012

Available online 4 January 2013

Abstract. The ordered patterns formed by microphase-separated block copolymer systems demonstrate periodic symmetry, and all periodic structures belong to one of 230 space groups. Based on this fact, a strategy of estimating the initial values of self-consistent field theory to discover ordered patterns of block copolymers is developed. In particular, the initial period of the computational box is estimated by the Landau-Brazovskii model as well. By planting the strategy into the whole-space discrete method, several new metastable patterns are discovered in diblock copolymers.

AMS subject classifications: 65M70, 76A15

Key words: Metastable patterns, diblock copolymers, self-consistent field theory (SCFT), space group theory, initial values.

1 Introduction

In the last decade, ordered patterns formed by block copolymers have attracted great attention. Block copolymers are composed of different chemical block chains. The self-assembly behavior of block copolymers is driven by various interactions among the different blocks, the volume fraction of blocks, and the topological constraint of the chain architecture. Ordered equilibrium patterns are a result of the delicate balance among these complex competing factors. Potential applications of these ordered patterns include lithographic templates for nanoparticle synthesis, photonic crystals and high density magnetic storage media [1]. Therefore, how to search for the ordered patterns becomes

*Corresponding author. *Email addresses:* jiangkai@pku.edu.cn (K. Jiang), chu.wang.pku@gmail.com (C. Wang), huangyq@xtu.edu.cn (Y. Huang), pzhang@pku.edu.cn (P. Zhang)

especially important for the development of nanotechnology using block copolymers. It also presents a complex and challenging problem for studying the phase behavior of the block copolymers [2].

In AB diblock copolymers, a number of ordered patterns have been discovered, such as lamellae (LAM), hexagonally packed cylinders (HPC), hexagonally perforated lamellae (HPL), spheres in body-centered-cubic (BCC) lattice, spheres in face-centered-cubic (FCC) lattice, bicontinuous double gyroid (DG), bicontinuous double diamond (DD) and *Fddd* patterns [3,4]. Among these rich ordered patterns, the metastable patterns play an important role. They often become the dominant state for the entire system and are observed over a range of time and size scales in phase transitions [5–7]. For example, metastable phase HPL is observed as an intermediate phase in LAM→DG transition [8]. Another important fact is that the metastable patterns in diblock copolymers may be stable in other polymeric systems. For example, the pattern A-15 in AB diblock copolymers is metastable, however, it is a stable pattern in AB_n graft diblock copolymers [9]. DD, HPL are the stable patterns in the blends of AB diblock copolymer and A homopolymer, and also metastable ones in AB diblock copolymer melt [10]. Therefore, it is important to develop an efficient strategy to capture as many ordered patterns as possible, including stable and metastable ones.

Theoretically, the SCFT provides a successful framework for studying the equilibrium phase behavior of block copolymers. By searching for the solutions of the self-consistent field equations, one can find the equilibrium ordered patterns of block copolymers. However, SCFT is a set of highly nonlinear equations with multi-solutions. The equations have a strong nonlocality that emerges from the connection of propagators and density, mean external fields. The solutions are also dependent on the interacting parameters and compositions. Finding all solutions of SCFT analytically is beyond today's technology. A successful alternative is to solve the self-consistent field equations numerically.

Generally, there are three main parts required to study nonlinear equations with multi-solutions: the initial values, the discrete schemes and the nonlinear iterative methods. Two kinds of numerical versions are developed to discretize the self-consistent field equations. The first type is the projective-space discrete method which discretizes equations in a special subspace based on specific problems. According to the specific pattern and its symmetric group in microphase-separated block copolymers, the self-consistent field equations can be expanded in terms of a set of symmetric basis functions [11]. This method is a powerful tool to analyze the phase behavior of the known phases. However, it is generally granted that this method is unable to discover new patterns. The second type is the whole-space discrete method whose approximated space is the whole space. This method can be carried out both in real space [12] and in Fourier-space [13]. It has also been demonstrated that the whole-space discrete methods are able to capture new patterns [12,13]. In recent years, an efficient pseudospectral method has been introduced to solve the modified diffusion equations in SCFT [14,15] for the whole-space discrete methods. It fully takes advantage of the best performance of real space and Fourier-space and reduces the computational complexity to $\mathcal{O}(N\log N)$, with the number of spectral modes

N , based on the Fast Fourier Transformation (FFT). Many iterative methods have been developed in order to find the saddle-points of the SCFT, such as mixing-type iterative methods [12, 16] and gradient-type iterative methods [17]. Among these methods, the Anderson mixing method [16, 18] and semi-implicit method [17] can accelerate convergence greatly.

The initial values not only influence the convergent properties of iterative procedures, but also the final morphology of solutions because of the presence of multiple solutions of the nonlinear self-consistent field equations. However, the initial value estimation has received less attention in previous research. Usually, random distributions are chosen to estimate initial distributions [12, 16], which is an inefficient strategy. To address this issue, we continue to develop more efficient strategies to estimate appropriate initial values based on our previous work [19]. It is noted that the patterns in microphase-separated block copolymers exhibit periodic symmetry and all periodic symmetric structures belong to one of 230 space groups. This research tries to apply the space group theory to the whole-space discrete methods to develop a strategy which has the potential to capture new patterns.

The rest of this paper is organized as follows: in Section 2 the SCFT of an incompressible diblock copolymer melt is introduced briefly. In Section 3, the numerical methods employed are discussed in detail, especially the strategy for estimating the initial values. The numerical results which demonstrate the efficiency of our proposed method will be shown in Section 4. Finally, the discussion and summary of the current study are given in Section 5.

2 Self-consistent field theory

In this section, we will give a brief introduction to the self-consistent field model for an incompressible diblock copolymer melt. Consider a system with volume V of n conformationally symmetric diblock copolymers each having A and B arms joined together with a covalent bond. The total degree of polymerization of a diblock copolymer is N , and the A -monomer fraction is f , correspondingly, the B -monomer fraction is $1-f$. The field-theoretic Hamiltonian for the incompressible diblock copolymer melt is [15, 20]

$$H = \frac{1}{V} \int d\mathbf{r} \left\{ -w_+(\mathbf{r}) + \frac{w_-^2(\mathbf{r})}{\chi N} \right\} - \log Q[w_+, w_-]. \quad (2.1)$$

where χ is the Flory-Huggins parameter to describe the interaction between segments A and B . The terms $w_+(\mathbf{r})$ and $w_-(\mathbf{r})$ can be viewed as fluctuating pressure and exchange chemical potential fields, respectively. The pressure field enforces the local incompressibility, while the exchange chemical potential is conjugate to the density operators. The function Q is the single chain partition function, which is computed according to

$$Q = \frac{1}{V} \int d\mathbf{r} q(\mathbf{r}, s) q^\dagger(\mathbf{r}, s), \quad \forall s \in [0, 1]. \quad (2.2)$$

The forward propagator $q(\mathbf{r},s)$ represents the probability weight that the chain of contour length s has its end at position \mathbf{r} . The variable s is used to parameterize each copolymer chain such that $s=0$ represents the tail of the A block and $s=f$ is the junction between the A and B blocks. From the flexible Gaussian chain model [20], $q(\mathbf{r},s)$ satisfies the modified diffusion equation (MDE)

$$\frac{\partial}{\partial s}q(\mathbf{r},s) = R_g^2 \nabla_{\mathbf{r}}^2 q(\mathbf{r},s) - w_K(\mathbf{r})q(\mathbf{r},s), \quad (2.3a)$$

$$w_K = \begin{cases} w_A = w_+ - w_-, & 0 \leq s \leq f, \\ w_B = w_+ + w_-, & f \leq s \leq 1, \end{cases} \quad (2.3b)$$

with the initial condition $q(\mathbf{r},0) = 1$ and R_g being the radius of gyration. The reverse propagator $q^\dagger(\mathbf{r},s)$, which represents the probability weight from $s = 1$ to $s = 0$, satisfies Eq. (2.3) only with the right-hand side multiplied by -1 . The initial condition is $q^\dagger(\mathbf{r},1) = 1$. The normalized segment density operators $\phi_A(\mathbf{r})$ and $\phi_B(\mathbf{r})$ follow from functional derivatives of Q with respect to w_A and w_B and the familiar factorization property of propagators

$$\phi_A(\mathbf{r}) = -\frac{V}{Q} \frac{\delta Q}{\delta w_A} = \frac{1}{Q} \int_0^f ds q(\mathbf{r},s) q^\dagger(\mathbf{r},s), \quad (2.4)$$

$$\phi_B(\mathbf{r}) = -\frac{V}{Q} \frac{\delta Q}{\delta w_B} = \frac{1}{Q} \int_f^1 ds q(\mathbf{r},s) q^\dagger(\mathbf{r},s). \quad (2.5)$$

By computing the first variations of the Hamiltonian with respect to fields w_+ and w_- , one can obtain the mean-field equations

$$\phi_A(\mathbf{r}) + \phi_B(\mathbf{r}) = 1, \quad (2.6)$$

$$\phi_A(\mathbf{r}) - \phi_B(\mathbf{r}) = \frac{2w_-(\mathbf{r})}{\chi N}. \quad (2.7)$$

Our objective is to compute as many equilibrium states as possible by solving the self-consistent field equations efficiently.

3 Numerical method

The SCFT models are a set of highly nonlinear and strongly nonlocal equations with multi-solutions and multi-parameters. Solutions for the equilibrium density distribution of different blocks, in turn, uniquely specify mean fields and other interesting physical quantities. For a fixed computational box, the common iteration procedure to solve SCFT includes the following steps:

Step 1 At the first step $i = 1$, give proper parameters χN , f , reasonable initial distributions of w_+^i , w_-^i , and the computational box.

Step 2 Solve MDEs (2.3) to determine q and q^\dagger for $0 \leq s \leq 1$. Use Eqs. (2.4)-(2.5) to obtain new density fields ϕ_A^i and ϕ_B^i .

Step 3 Update fields w_+^{i+1} and w_-^{i+1} by Eqs. (2.6)-(2.7) through iterative methods.

Step 4 The procedure is repeated from **Step 2** until the given convergent condition is reached.

From the iterative procedure, there are three main parts required for solving the set of nonlinear equations numerically. The first part is to determine the appropriate initial values, including reasonable initial distributions of mean-fields or densities, proper parameters (Flory-Huggins interaction parameters and volume fractions), and initial computational boxes. The second part is the special discrete schemes for the equation system and efficient numerical schemes for MDE (2.3). The third part is the iterative method to find the equilibrium states.

3.1 Discrete SCFT in Fourier-space

Since equilibrium ordered patterns formed by block copolymers are periodic, we consider periodic boundary conditions and discretize the self-consistent field equations in the whole-space. All spatial varying functions with periodic conditions, $\psi(\mathbf{r})$, are expanded as Fourier series

$$\psi(\mathbf{r}) = \sum_{\{\mathbf{G}\}} \psi(\mathbf{G}) e^{i\mathbf{G}\cdot\mathbf{r}}, \quad (3.1)$$

where $\{\mathbf{G}\} = \{\mathbf{G}_{mnk} | m\mathbf{b}_1 + n\mathbf{b}_2 + k\mathbf{b}_3\}$, $m, n, k \in \mathbf{Z}$, and wave vectors \mathbf{b}_1 , \mathbf{b}_2 and \mathbf{b}_3 are the primitive vectors of the reciprocal lattice. The corresponding primitive vectors in physical space are \mathbf{a}_1 , \mathbf{a}_2 , \mathbf{a}_3 . These two sets of primitive vectors satisfy $\mathbf{a}_i \cdot \mathbf{b}_j = 2\pi\delta_{ij}$, where $i, j = 1, 2, 3$. One can always choose a proper coordinate system such that $b_{12} = 0$, $b_{13} = 0$, $b_{23} = 0$, and $b_{11} \neq 0$, $b_{22} \neq 0$, $b_{33} \neq 0$. For brevity, the element of $\{\mathbf{G}\}$ is written as \mathbf{G} instead of \mathbf{G}_{mnk} , and $\mathcal{B} = (\mathbf{b}_1, \mathbf{b}_2, \mathbf{b}_3)$. More details on discrete schemes can be found in [19].

Here, we define

$$Error = \max \left\{ \max_{\{\mathbf{G}\}} \left| \left(\frac{\delta H}{\delta w_+} \right)_{\mathbf{G}} \right|, \max_{\{\mathbf{G}\}} \left| \left(\frac{\delta H}{\delta w_-} \right)_{\mathbf{G}} \right| \right\} \quad (3.2)$$

to measure the error toleration. Moreover, $\left(\frac{\delta H}{\delta w_+} \right)_{\mathbf{G}}$ and $\left(\frac{\delta H}{\delta w_-} \right)_{\mathbf{G}}$ are the Fourier coefficients of corresponding first order variations of the effective Hamiltonian (2.1).

3.2 Initial values

In essence, the SCFT is a nonlinear and nonlocal variational problem with multi-solutions and multi-parameters. For nonlinear problems with multi-solutions, the initial values play a crucial role. They not only influence the algorithm's efficiency, but also decide the final morphology of solutions. The initial values in solving SCFT include three parts:

the initial estimation of field or density distribution, proper parameters (Flory-Huggins interaction χ and volume fractions f), and the initial computational box.

Recently, there has been much research about the parameters of stable patterns in diblock copolymers. A powerful tool to study the stability of a pattern is the phase diagram [11, 15]. Therefore, we will not discuss this problem, and focus on how to estimate the initial distribution and computational box in this paper.

3.2.1 Generate the initial distribution

In general, there is no universal method to generate initial values for a complex non-linear variational problem with multi-solutions. Fortunately, the patterns in microphase-separated copolymer systems can exhibit periodic symmetry described by the space group theory. We plant this theory into the whole-space discrete methods to search for patterns based on self-consistent field calculations. The basic idea of the strategies of generating initial distributions using space groups comes from our previous research [19]. In this paper, we will further develop and summarize the strategy to discover new patterns feasibly.

In the beginning, we give some discussion about the relationship between the space group theory and periodic patterns. Firstly, different patterns may belong to the same space group. For example, BCC and BCC₃ both belong to $Im\bar{3}m$ and single gyroid (SG) and alternating gyroid in ABC triblock copolymers both belong to $I4_132$. The different patterns with the same space group are distinguished by the strongest modulation of different reciprocal vectors, corresponding to the primary peaks in scattering experiments. For example, the primary wave vectors of BCC are the [110] family of reciprocal lattice vectors, whereas the primary ones of BCC₃ are [210]. Secondly, the space group theory can reveal the symmetry in Fourier-space, such as the relationship of the moduli and signs of Fourier coefficients. It greatly reduces the possibilities of nonzero Fourier coefficients. However, it can not point out the special values and signs of Fourier coefficients. The solution to identify the signs of Fourier coefficients in practical implementations is to go through the remaining possibilities. Three steps are summarized to estimate the initial distributions for a possible pattern:

Step 1 Identify the space group of the possible pattern;

Step 2 Identify the primary reciprocal vectors which yield the final morphologies;

Step 3 Identify the signs of the Fourier coefficients of previously decided primary reciprocal vectors.

From our experience, the specific value of initial Fourier coefficients has little impact on the final morphologies.

One can directly obtain the initial distributions for the known patterns, especially for the patterns analyzed by experiments or theories. The space groups and corresponding primary reciprocal vectors have been identified for some common patterns, such as the LAM, HPC, HPL, BCC, FCC, DD, DG and $Fddd$ [21–24]. For example, the strongest

Table 1: The initial primary reciprocal vectors of ordered phases for AB linear diblock copolymers.

Patterns (Space group)	The initial reciprocal vectors \mathbf{G}_{mnk}
Primitive cubic Spheres ($Pm\bar{3}m$)	$(\pm 1, 0, 0), (0, \pm 1, 0), (0, 0, \pm 1),$ $(\pm 1, \pm 1, 0), (\pm 1, 0, \pm 1), (0, \pm 1, \pm 1)$
BCC ($Im\bar{3}m$)	$(0, \pm 1, \pm 1), (\pm 1, 0, \pm 1), (\pm 1, \pm 1, 0)$
FCC ($Fm\bar{3}m$)	$(111), (\bar{1}\bar{1}\bar{1}), (\bar{1}11), (1\bar{1}\bar{1})$
A-15 ($Pm\bar{3}n$)	$(\bar{2}\bar{1}0), (210), (\bar{2}\bar{1}0), (\bar{2}10), (\bar{1}20)^a, (1\bar{2}0)^a,$ $(120)^a, (\bar{1}\bar{2}0)^a, (0\bar{2}1), (\bar{2}01)^a, (021), (201)^a,$ $(\bar{1}02), (0\bar{1}2)^a, (012)^a, (102)$
PS ₅ ($Pm\bar{3}m(5)$)	$(\pm 1, 0, \pm 2)^a, (\pm 1, \pm 2, 0)^a, (\pm 2, 0, \pm 1)^a,$ $(\pm 2, \pm 1, 0)^a, (0, 0, \pm 3), (0, \pm 3, 0),$ $(\pm 3, 0, 0), (0, \pm 1, \pm 2)^a, (0, \pm 2, \pm 1)^a,$
BCC ₃ ($Im\bar{3}m(3)$)	$(\pm 2, \pm 1, \pm 1), (\pm 1, \pm 2, \pm 1), (\pm 1, \pm 1, \pm 2)$
Double Gyroid ($Ia\bar{3}d$)	$(\bar{2}11)^a, (\bar{2}\bar{1}\bar{1})^a, (2\bar{1}\bar{1})^a, (211), (1\bar{2}1), (12\bar{1}),$ $(\bar{1}\bar{2}\bar{1})^a, (\bar{1}21)^a, (11\bar{2}), (1\bar{1}2)^a, (\bar{1}12), (\bar{1}\bar{1}\bar{2})$
Single Gyroid ($I4_132$)	$(011)^I, (0\bar{1}\bar{1}), (0\bar{1}\bar{1}), (0\bar{1}\bar{1})^{I,a}, (101), (10\bar{1})^I,$ $(110)^{I,a}, (1\bar{1}0), (\bar{1}01)^{I,a}, (\bar{1}0\bar{1}), (\bar{1}10)^I, (\bar{1}\bar{1}0)^I$
Double Diamond ($Pn\bar{3}m$)	$(\bar{1}01), (011), (0\bar{1}\bar{1})^a, (101)^a, (\bar{1}\bar{1}0)^a, (\bar{1}\bar{1}0)^a,$ $(110), (\bar{1}\bar{1}0), (\bar{1}\bar{1}\bar{1})^a, (111)^a, (\bar{1}\bar{1}\bar{1})^a, (\bar{1}\bar{1}\bar{1})^a$
Single Diamond ($Fd\bar{3}m$)	$(211), (\bar{2}\bar{1}\bar{1})^a, (2\bar{1}\bar{1})^a, (\bar{2}\bar{1}\bar{1}), (121), (\bar{1}\bar{2}\bar{1}),$ $(\bar{1}\bar{2}\bar{1})^a, (\bar{1}\bar{2}\bar{1})^a, (112), (\bar{1}\bar{1}2)^a, (1\bar{1}\bar{2}), (\bar{1}\bar{1}\bar{2})^a,$
Hexagonally Packed Cylinders ($P6mmm$)	$(01\bar{1}), (0\bar{1}\bar{1}), (10\bar{1}),$ $(1\bar{1}0), (\bar{1}01), (\bar{1}10)$
Tetragonally Packed Cylinders ($I4mmm$)	$(\bar{1}\bar{1}0), (1\bar{1}0),$ $(1\bar{1}0), (\bar{1}\bar{1}0)$
Hexagonally Perforated Lamellae ($P6_3mmc$)	$(10\bar{1}), (101), (01\bar{1}),$ $(011), (110)$
Tetragonally Perforated Lamellae ($R\bar{3}m$)	$(200) (\bar{2}00)$ $(111) (\bar{1}\bar{1}\bar{1}) (\bar{1}\bar{1}\bar{1}) (\bar{1}\bar{1}\bar{1})$
$Fddd (O^70)$	$(111)^a, (1\bar{1}\bar{1}), (\bar{1}\bar{1}\bar{1}), (1\bar{1}\bar{1}),$ $(022)^a, (0\bar{2}\bar{2}), (004)$

^a denotes the sign of Fourier coefficients is opposite.

^I denotes the Fourier coefficients only have an imaginary part.

modulation of $Fddd$ pattern occurs at $[111]$, $[022]$ and $[004]$ reciprocal vectors in experiments [4]. Ranjan *et al.* [24] have developed a Landau theory to study the stability of the $Fddd$ phase through analyzing these primary reciprocal vectors. The initial distributions of the known patterns analyzed by theories can also be obtained. Erukhimovich's weak segregation theory [23] predicts BCC₃ pattern (space group $Im\bar{3}m$) and single gyroid (SG) pattern (space group $I4_132$), and gives the primary family reciprocal lattice vectors. We utilize the information as initial distributions in self-consistent field simulations and generate those corresponding patterns in numerical results. These reciprocal vectors are summarized in Table 1.

The space groups of some patterns have been identified, while there is no experiments and theories to analyze the patterns. We can also use the crystal structure factor tables to estimate corresponding initial distributions. For example, the spherical pattern, A-15, with space group $Pm\bar{3}n$, is a stable phase in AB_n ($n \geq 2$) miktoarm star copolymers systems [9]. So far there is no theory to analyze the pattern and give the primary reciprocal vectors in the relevant literature. However we can find the initial reciprocal vectors by the structure factor table of space group $Pm\bar{3}n$ to determine the primary vectors and signs of Fourier coefficients [25], as shown in Table 1. In the same way, the primary initial reciprocal vectors of the single diamond (SD) pattern with space group $Fd\bar{3}m$ are summarized in Table 1.

The method is able to discover new patterns. Since different patterns may belong to the same space group, their morphologies can be determined by the primary wave vectors. From this principle, we can use different dominant reciprocal vectors, but belonging to the same space group, to obtain different patterns. We take the space group $Pm\bar{3}m$ as an example. The dominant wave vectors of primitive cubic spheres (PS) are [100] with $Pm\bar{3}m$ symmetry. The higher order reciprocal vectors can be also used as initial vectors to search for new patterns. We find that the 5th order diffraction, [210], can determine a new pattern PS_5 , whose morphology can be found in Section 4.1. The initial vectors are listed in Table 1.

The approximated space of our employed discretization scheme is the whole space. Therefore, one can use the obtained pattern as an initial distribution to discover new patterns through adjusting parameters. We will give numerical examples to verify this viewpoint in Section 4.1.

3.2.2 Estimate the initial computational box

We use the Landau-Brazovskii model to analyze the period of the computational box because of the complexity of SCFT. In fact, the Landau-Brazovskii model is an approximated theory of SCFT in weak segregation [21,26]. The free energy density functional of the Landau-Brazovskii model is

$$f_0[\phi(\mathbf{r}_0)] = \frac{1}{V_0} \int d\mathbf{r}_0 \left\{ \frac{\xi_0^2}{8q_0^2} [(\nabla_{\mathbf{r}_0}^2 + q_0^2)\phi(\mathbf{r}_0)]^2 + \frac{\tau_0}{2} [\phi(\mathbf{r}_0)]^2 - \frac{\gamma_0}{3!} [\phi(\mathbf{r}_0)]^3 + \frac{\lambda_0}{4!} [\phi(\mathbf{r}_0)]^4 \right\}, \quad (3.3)$$

where $\phi(\mathbf{r}_0)$ is the order parameter, which is the density deviation of a kind of monomer from the disordered phase; V_0 is the system volume; ξ_0 is the bare correlation length; q_0 is the critical wave length; τ_0 is the reduced temperature; γ_0 and $\lambda_0 > 0$ are phenomenological constants. Rescaling the free energy functional by

$$\mathbf{r} = q_0 \mathbf{r}_0, \quad V = q_0^3 V_0, \quad f = \frac{f_0}{\lambda_0}, \quad \xi^2 = \frac{q_0^2 \xi_0^2}{4\lambda_0}, \quad \tau = \frac{\tau_0}{\lambda_0}, \quad \gamma = \frac{\gamma_0}{\lambda_0}, \quad (3.4)$$

the free energy density functional becomes

$$f[\phi(\mathbf{r})] = \frac{1}{V} \int d\mathbf{r} \left\{ \frac{\xi^2}{2} [(\nabla_{\mathbf{r}}^2 + 1)\phi(\mathbf{r})]^2 + \frac{\tau}{2} [\phi(\mathbf{r})]^2 - \frac{\gamma}{3!} [\phi(\mathbf{r})]^3 + \frac{1}{4!} [\phi(\mathbf{r})]^4 \right\}. \quad (3.5)$$

The order parameter $\phi(\mathbf{r})$ is expanded in Fourier-space as Eq. (3.1), and the free energy density functional can be written as

$$f[\phi(\mathbf{r}), \mathcal{B}] = g(\phi(\mathbf{G})) + \frac{1}{2} \sum_{\mathbf{G}} [\xi^2 (1 - |\mathbf{G}|^2)^2 + \tau] \phi(\mathbf{G}) \phi(-\mathbf{G}), \quad (3.6)$$

where

$$g(\phi(\mathbf{G})) = -\frac{\gamma}{3!} \sum_{\mathbf{G}_1 + \mathbf{G}_2 + \mathbf{G}_3} \phi(\mathbf{G}_1) \phi(\mathbf{G}_2) \phi(\mathbf{G}_3) + \frac{1}{4!} \sum_{\mathbf{G}_1 + \mathbf{G}_2 + \mathbf{G}_3 + \mathbf{G}_4} \phi(\mathbf{G}_1) \phi(\mathbf{G}_2) \phi(\mathbf{G}_3) \phi(\mathbf{G}_4). \quad (3.7)$$

It should be noted that only the Laplace term in Landau-Brazovskii free energy density functional is related to the period of the computational box. Minimizing the free energy functional with respect to the period of the computational box,

$$\frac{\partial f}{\partial b_{ij}} = 0, \quad i = 1, 2, 3, \quad j \leq i, \quad (3.8)$$

we can obtain the dimensionless optimum period of the computational box \mathbf{b}_j , $j = 1, 2, 3$. Note the rescale formula (3.4), the optimum period of the computational box in real space satisfies

$$\mathbf{a}_i \cdot \mathbf{b}_j = 2\pi \delta_{ij}, \quad \mathbf{a}_i = \mathbf{a}_i / q_0, \quad i, j = 1, 2, 3. \quad (3.9)$$

In order to obtain the optimal period of the computational box, we consider the quadratic coefficient, $S(\mathbf{G})$, in Leibler's mean field theory which is also an approximated theory of SCFT [21, 26],

$$S(\mathbf{G}) = \psi(\mathbf{G}, f) - 2\chi N, \quad (3.10)$$

and

$$\psi(\mathbf{G}, f) = g(|\mathbf{G}|^2, 1) / \{g(|\mathbf{G}|^2, f)g(|\mathbf{G}|^2, 1-f) - (1/4)[g(|\mathbf{G}|^2, 1) - g(|\mathbf{G}|^2, f) - g(|\mathbf{G}|^2, 1-f)]^2\}, \quad (3.11)$$

where $g(x, s)$ is the Debye function

$$g(x, s) = \frac{2}{x^2} (e^{-xs} + xs - 1). \quad (3.12)$$

The spinodal, or stability limit, of the homogeneous phase of diblock copolymers towards microphase separation is obtained from the relation [20]

$$S(\mathbf{G}_m(f)) = \psi(\mathbf{G}_m(f), f) - 2\chi N, \quad (3.13)$$

where $\mathbf{G}_m(f)$ is the minimum point of $\psi(\mathbf{G}_m(f), f)$ at fixed composition f , and $(\chi N)_{spinodal} = (1/2)\psi(\mathbf{G}_m(f), f)$. Then

$$q_0^2 = \frac{|\mathbf{G}_m(f)|^2}{R_g^2}. \quad (3.14)$$

Therefore, we can use Eq. (3.9) to obtain the initial period of the computational box.

3.3 Numerical schemes to solve MDE

Here, we use a pseudospectral method and fourth-order accurate Adams-Bashford scheme [15] to solve MDE (2.3)

$$\begin{aligned} & \frac{25}{12}q^{j+1} - 4q^j + 3q^{j-1} - \frac{4}{3}q^{j-2} + \frac{1}{4}q^{j-3} \\ & = \Delta s \left[\nabla^2 q^{j+1} - w_A (4q^j - 6q^{j-1} + 4q^{j-2} - q^{j-3}) \right]. \end{aligned} \quad (3.15)$$

In Fourier-space, the Adams-Bashford method is written as

$$\begin{aligned} & \frac{25}{12}q_{\mathbf{G}}^{j+1} - 4q_{\mathbf{G}}^j + 3q_{\mathbf{G}}^{j-1} - \frac{4}{3}q_{\mathbf{G}}^{j-2} + \frac{1}{4}q_{\mathbf{G}}^{j-3} \\ & = -\Delta s |\mathbf{G}|^2 q_{\mathbf{G}}^{j+1} - \Delta s \sum_{\mathbf{G}_1} \left[w_{A, \mathbf{G}-\mathbf{G}_1} (4q_{\mathbf{G}_1}^j - 6q_{\mathbf{G}_1}^{j-1} + 4q_{\mathbf{G}_1}^{j-2} - q_{\mathbf{G}_1}^{j-3}) \right]. \end{aligned} \quad (3.16)$$

The required initial values are computed by the second-order operator splitting scheme [14, 27]. The Laplacian term can be calculated in Fourier-space easily, and the convolution sum is the scale multiplication in real space. The Fourier-space and real space are connected by FFT.

3.4 Iterative method

The iterative methods to update the fields are dependent on the information provided by SCFT. An important fact is that the effective Hamiltonian (2.1) can reach its local minima along the exchange chemical field w_- , and reach the maxima along the pressure field w_+ [20]. Therefore, the gradient-type algorithms can be applied in the iteration procedure to search for equilibrium points in numerical simulations. An efficient iterative method, a semi-implicit method [17], is chosen in our simulation, which can be expressed in Fourier-space as

$$\frac{\mu_{+, \mathbf{G}}^{j+1} - \mu_{+, \mathbf{G}}^j}{\Delta t} = -\hat{g}(\mathbf{G})\mu_{+, \mathbf{G}}^{j+1} + \frac{\delta h[\mu_{+, \mathbf{G}}^j, \mu_{-, \mathbf{G}}^j]}{\delta \mu_{+, \mathbf{G}}} + \hat{g}(\mathbf{G})\mu_{+, \mathbf{G}}^j, \quad (3.17)$$

$$\frac{\mu_{-, \mathbf{G}}^{j+1} - \mu_{-, \mathbf{G}}^j}{\Delta t} = -\frac{2}{\chi N}\mu_{-, \mathbf{G}}^{j+1} - \frac{\delta h[\mu_{+, \mathbf{G}}^{j+1}, \mu_{-, \mathbf{G}}^j]}{\delta \mu_{-, \mathbf{G}}} + \frac{2}{\chi N}\mu_{-, \mathbf{G}}^j, \quad (3.18)$$

where

$$\hat{g}(\mathbf{G}) = \frac{2}{\mathbf{G}^4} \left(e^{-\mathbf{G}^2} + \mathbf{G}^2 - 1 \right). \quad (3.19)$$

3.5 Adjust computational box

The accurate value of the effective Hamiltonian of SCFT depends not only on the fields, but also on the period of the computational box. Therefore, the computational box should be adjusted adaptively in terms of different ordered patterns. We use the steepest descent method to optimize the computational box \mathcal{B} [19]. If \mathcal{B} is one of the solutions, the first derivatives of the effective Hamiltonian with respect to \mathbf{b}_j , $j=1,2,3$, should be zero. The computational box can be updated by

$$\mathbf{b}_j^{i+1} = \mathbf{b}_j^i - \alpha \frac{\partial H}{\partial \mathbf{b}_j}, \quad (3.20)$$

where $\partial H / \partial \mathbf{b}_j$ is calculated numerically, and the iterative step α is calculated by linear search algorithms.

Therefore, the integrated iteration procedure, including updating the field functions and computational box, contains the following steps:

Step 1 Give proper parameters χ , f , reasonable initial distributions of w_A , w_B , and the computational box, and set $m=1$, calculate the effective Hamiltonian H_m .

Step 2 Fix the computational box \mathcal{B} , calculate field functions by the iteration procedure as described in the beginning of the section.

Step 3 Adjust \mathcal{B} by the method described in Section 3.5, calculate effective Hamiltonian H_{m+1} .

Step 4 If $|H_{m+1} - H_m| > \varepsilon$, set $H_m = H_{m+1}$, $m = m+1$, goto **Step 2**, else end the iteration procedure.

In the following simulations, we will choose the entire iteration procedure to calculate self-consistent field equations. The period of the computational box is optimized concurrently with the fields by minimizing the effective Hamiltonian during the iteration procedure.

4 Numerical results

4.1 Discovery of patterns

Applying these initial distributions analyzed in Section 3.2.1 in SCFT calculations, the corresponding ordered patterns have been captured in simulations. The selected metastable patterns can be found in Fig. 1. We also find a novel spherical pattern S-13, as shown in Fig. 1(q), if the higher order reciprocal vectors with space group $Pm\bar{3}m$ are input as initial vectors. It is a more close packed spherical structure than the A-15 pattern,

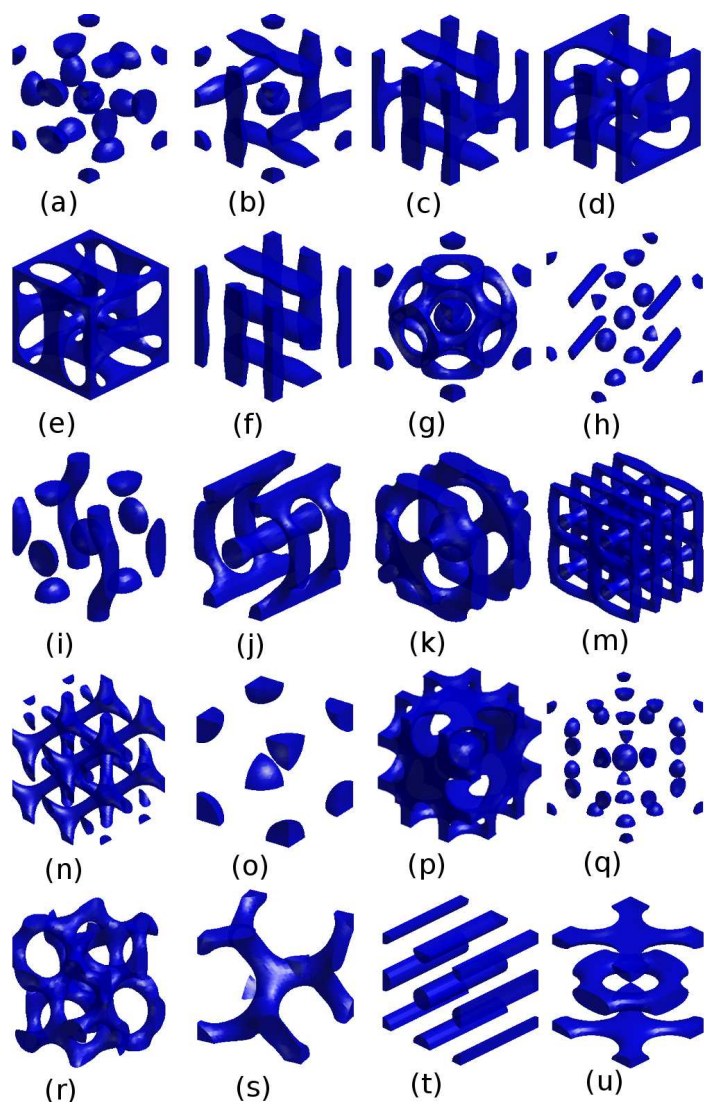


Figure 1: Captured ordered metastable patterns of AB diblock copolymers based upon self-consistent field theory. There are 20 patterns: (a) A-15, (b) A15Cyl, (c) A15CylNet, (d) A15Netwok, (e) A15NetwokBox, (f) AnisoCyl, (g) BCC₃, (h) C+S, (i) Helix+S, (j) Nwt+C, (k) Nwt+S, (l) PL+C, (m) DD, (n) PS, (o) PS₅, (p) S-13, (r) SD, (s) SG, (t) TPC, (u) TPL.

and includes 13 spheres in a period of the computational box. However, the metastable pattern is only found in a few regions of the phase space, such as the neighborhood of $[\chi N, f] = [15.0, 0.29]$.

Since the approximated space of our method is the whole space, we can use the discovered pattern as initial values to discover new patterns through adjusting parameters. Next, we give an example to check our approach. By setting the convergence data of the A-15 pattern as initial values and fixing $\chi N = 15.0$, we can obtain different patterns at

different volume fraction f . As the volume fraction f increases, the final morphologies are successively A-15, A15Cyl, A15Cylnet, A15Network and A15NetworkBox, as shown in Fig. 1(a-e). The morphology transition is dominated by the volume fraction f . When f increases, the spheres on the face of the A-15 pattern will blend into cylinders which forms the A15Cyl pattern. As the volume fraction f further increases, the body-centered sphere grows into a cylinder and connects with the cylinders on the face of the cubic lattice. Fig. 2 gives the effective Hamiltonian of the set of patterns as a function of volume fraction f . The relative energy curves of stable phases are also shown in order to describe the difference of the effective Hamiltonian between metastable and stable patterns. The exiting areas of A-15, A15Cyl, A15Cylnet, A15Network and A15NetworkBox are $0.28 \leq f \leq 0.35$, $0.33 \leq f \leq 0.36$, $0.355 \leq f \leq 0.39$, $0.36 \leq f \leq 0.41$, and $0.41 \leq f \leq 0.50$, respectively.

Except for the above patterns, a large number of ordered patterns have been discovered in our simulations with the captured patterns as initial values, including network and spheres (Nwt+S) (Fig. 1(k)), network and cylinders (Nwt+C) (Fig. 1(j)), perforated lamellar and cylinders (PL+C) (Fig. 1(m)), helix and spheres (Helix+S) (Fig. 1(i)), cylinders and spheres (C+S) (Fig. 1(h)), BCC₃ (Fig. 1(g)), and PS₅ (Fig. 1(p)). Among these patterns, a novel cylindrical pattern in anisotropic arrangement lattice (AnisoCyl) has been discovered, as shown in Fig. 1(f).

In order to present the relative stability between these metastable patterns and the known stable phases, the energy images from the value of the homogeneous phase as a function of the volume fraction f as well as the exiting area at $\chi N = 15.0$, are shown in Fig. 3. Some metastable patterns with large energy values compared to other patterns are not shown in these energy plots, such as that of BCC₃ in the region of $0.32 \leq f \leq 0.50$, PS in the region of $0.29 \leq f \leq 0.33$, and PS₅ in the region of $0.36 \leq f \leq 0.49$. From these energy plots, one can find that the energy difference decreases as the diblock copolymer becomes more asymmetric.

Nevertheless, the approach using the primary reciprocal vectors as initial values applies to the weakly segregated system. Certainly, more reciprocal vectors can be used as initial estimate for strongly-segregated systems. However, it greatly increases the difficulty of determining the initial distributions because the complexity of the signs of Fourier coefficients will grow very rapidly. An alternative is to set the convergence results in weak segregation as initial distributions for the strongly-segregated systems.

Up to now, the strategy to estimate initial values based on the space group theory is carried out in Fourier-space. It should be pointed out that the approach can be applied in real space methods, which can be demonstrated by the following example. For the SG pattern, the initial value in real space is

$$\begin{aligned} \phi(\mathbf{r}) = & \phi_{011} \sin(y+z) + \phi_{0\bar{1}\bar{1}} \cos(y-z) + \phi_{0\bar{1}1} \cos(-y+z) - \phi_{0\bar{1}\bar{1}} \sin(-y-z) \\ & + \phi_{101} \cos(x+z) + \phi_{10\bar{1}} \sin(x-z) - \phi_{110} \sin(x+y) + \phi_{1\bar{1}0} \cos(x-y) \\ & - \phi_{\bar{1}01} \sin(-x+z) + \phi_{\bar{1}0\bar{1}} \cos(-x-z) + \phi_{\bar{1}10} \sin(-x+y) + \phi_{\bar{1}\bar{1}0} \sin(-x-y). \end{aligned} \quad (4.1)$$

The coefficients in Eq. (4.1) are all positive.

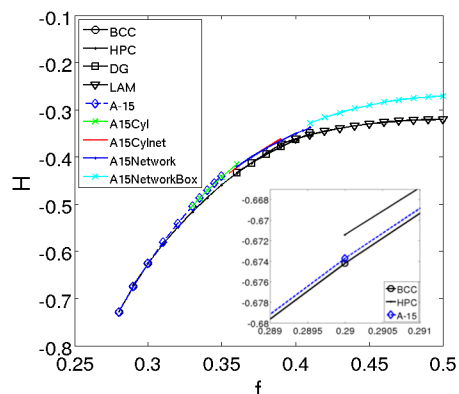


Figure 2: The effective Hamiltonian H as a function of f for fixed $\chi N = 15.0$ through setting the convergence result of A-15 patterns as initial values.

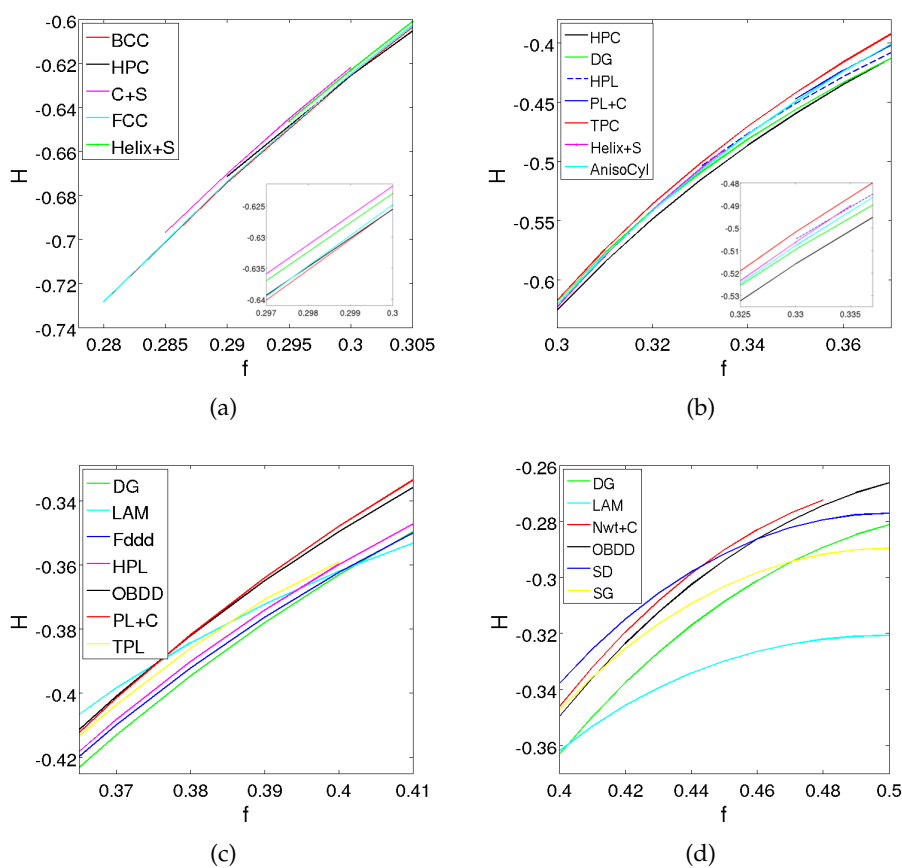


Figure 3: Energy curve of the metastable patterns and stable patterns from the value of homogeneous phase as a function of the volume fraction f as well as the exiting area for fixed $\chi N = 15.0$. (a) $0.28 \leq f \leq 0.305$. (b) $0.30 \leq f \leq 0.37$. (c) $0.365 \leq f \leq 0.41$. (d) $0.40 \leq f \leq 0.50$.

4.2 Period of computational box

Theoretically, the initial computational box can be estimated by Eq. (3.9) from the Landau-Brazovskii model. However, we do not know all nonzero Fourier coefficients $\phi(\mathbf{G})$ when calculating b_{opt} in Eq. (3.8). One solution is using the initial primary reciprocal vectors \mathbf{G} listed in Table 1 to estimate the initial computational box, especially for those patterns described by one family of reciprocal lattice vectors, such as DG, BCC, BCC₃. We take DG pattern as an example to demonstrate how to calculate the initial period structure. The initial vectors of DG are [211], we can then use the index to calculate the computational box by Eqs. (3.8)-(3.9). The period of the computational boxes by theoretical prediction has been summarized in Table 2. Meanwhile, the computational boxes can be adjusted during the iteration procedure. The final numerical results about the period of the computational boxes are also given in Table 2. From the results, one can find that the period of the computational box of theoretical prediction is a good approximation to the precise computational box in SCFT simulations.

Table 2: Theoretical prediction and simulation results of the period of the computational box.

Patterns	$[\chi N, f]$	Theory(R_g)	Simulation(R_g)
LAM*	[12.0, 0.45]	4.5586	4.8138
PS	[15.0, 0.30]	3.1262	3.4552
BCC	[11.4, 0.40]	4.5326	4.5856
FCC	[15.0, 0.28]	4.1014	5.7519
A-15	[30.0, 0.18]	6.5452	7.2642
HPC	[12.0, 0.40]	4.5326	4.8868
DG	[12.0, 0.43]	7.8814	8.3460
SG	[12.0, 0.43]	4.5503	4.6661
BCC ₃	[14.0, 0.40]	7.8506	8.6997
TPC	[20.0, 0.30]	3.1262	3.7759
DD	[14.0, 0.40]	4.5326	5.3149
SD	[14.0, 0.40]	7.8506	8.9345
HPL	[14.0, 0.40]	4.5326	5.0126
TPL	[15.0, 0.37]	6.3752	6.8413
PC	[20.0, 0.30]	7.6576	9.8259

The primary reciprocal vector for LAM* is (110).

Since the Landau-Brazovskii model is a weakly-segregated theory, the above results are valid near the disordered-ordered region. As shown in Fig. 4(a), when the interaction is weak, the results of simulation are consistent with the theoretical prediction for different compositions. As the interaction enhances, the gap between the theoretical predictions and simulation results becomes increasingly wider. However, the period of the computational box has a continuous change as interactions parameter χN becomes large, as shown in Fig. 4(b). Therefore, it still presents a fine initial computational box in strong segregation by the results of weakly-segregated systems.

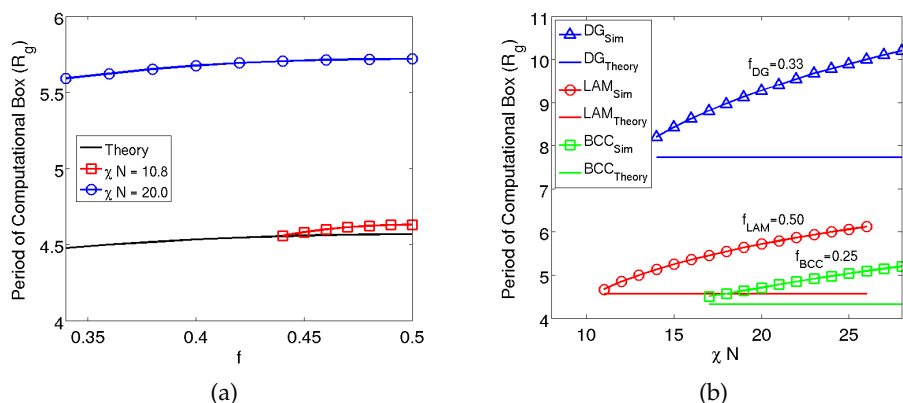


Figure 4: The theoretical prediction and numerical results on the period of the computational box in units of the radius of gyration R_g . The (110) reciprocal vector is used as initial values for LAM. (a) The period of the computational box is a function of the composition f at different χN for LAM pattern. (b) The period of the computational box is a function of χN with fixed composition f for different patterns.

5 Discussion and summary

We have developed and examined a method to discover ordered patterns by solving the self-consistent field equations for diblock copolymers numerically. Our strategy is to estimate the initial distributions of the field in the whole space calculations using the space group theory. In particular, the initial distributions can be obtained from experimental data or theoretical results directly, or from crystal structure factor tables. We also note that the different patterns may belong to the same space group, distinguished by different primary reciprocal vectors that can be used to capture different patterns. Since the approximated space is the whole space, the strategy can be used to discover new patterns by adjusting the parameters. By these strategies, many novel patterns have been discovered, as shown in Fig. 1, which greatly enriches the set of ordered patterns in block copolymers. These newly discovered patterns are metastable in diblock copolymers, however, those patterns with relatively low effective Hamiltonians may be stable in other neat block copolymer melts or blends.

Our strategy is different from Matsen-Schick's method (MSM) [11]. MSM is a special projective-space algorithm which adds the symmetric information to basis functions in calculation procedures. The fast algorithm, such as FFT, cannot be applied to this method directly. The major disadvantage of MSM is that it cannot be used to discover new patterns straightforwardly. At the same time, MSM is also faced with the challenge of initial values. The signs of Fourier coefficients in MSM also have been determined in practical implementation [19]. On the contrary, our strategy only needs to add a little symmetric information into the initial estimation, and it is based on the whole-space discrete method. It is more adaptive and flexible for discovering new patterns with less computational effort. We should point out that the work of [19] is one of the starting points in

our study to choose the initial distribution of field functions. Here, we continue to develop and summarize the strategy to screen initial values, and examine the availability of discovering new metastable patterns. Especially, the approach of estimating the initial computational box is given analytically through the Landau-Brazovskii model. Meanwhile, we believe that the initial values and these discovered metastable patterns will be of benefit to the studies of other polymeric systems.

Acknowledgments

The authors express appreciation to the anonymous referees whose suggestions resulted in a number of improvements to the paper. The work of P. Zhang is supported by grants from National Natural Science Foundation of China (50930003). The work of the Y. Huang was supported in part by the Key Project of National Natural Science Foundation of China (Grant No. 11031006), and the Natural Science Foundation of Hunan Province (Grant No. 10JJ7001). C. Wang is supported by Junzheng Foundation of Peking University. K. Jiang is supported by Visit Project of Beijing International Center for Mathematical Research and China Postdoctoral Science Foundation (Grant No. 2011M500179).

References

- [1] C. Park, J. Yoon, and E.L. Thomas. Enabling nanotechnology with self assembled block copolymer patterns. *Polymer*, 44(22):6725–6760, 2003.
- [2] T.P. Lodge. Block copolymers: past successes and future challenges. *Macromolecular Chemistry and Physics*, 204(2):265–273, 2003.
- [3] M.W. Matsen. The standard Gaussian model for block copolymer melts. *Journal of Physics: Condensed Matter*, 14:R21–R47, 2002.
- [4] M.I. Kim, T. Wakada, S. Akasaka, S. Nishitsuji, K. Saijo, H. Hasegawa, K. Ito, and M. Takenaka. Stability of the Fddd phase in diblock copolymer melts. *Macromolecules*, 41(20):7667–7670, 2008.
- [5] S.Z.D. Cheng and A. Keller. The role of metastable states in polymer phase transitions: Concepts, principles, and experimental observations. *Annual Review of Materials Science*, 28(1):533–562, 1998.
- [6] W. E, B. Engquist, X. Li, W. Ren, and E. Vanden-Eijnden. Heterogeneous multiscale methods: a review. *Communications in Computational Physics*, 2(3):367–450, 2007.
- [7] N.M. Abukhdeir and A.D. Rey. Simulation of spherulite growth using a comprehensive approach to modeling the first-order isotropic/smectic-A mesophase transition. *Communications in Computational Physics*, 7(2):301–316, 2010.
- [8] X. Cheng, L. Lin, W. E, P. Zhang, and A.C. Shi. Nucleation of ordered phases in block copolymers. *Physical Review Letters*, 104(14):148301, 2010.
- [9] G.M. Grason, B.A. DiDonna, and R.D. Kamien. Geometric theory of diblock copolymer phases. *Physical Review Letters*, 91(5):58304, 2003.
- [10] M.W. Matsen. Stabilizing new morphologies by blending homopolymer with block copolymer. *Physical Review Letters*, 74(21):4225–4228, 1995.

- [11] M.W. Matsen and M. Schick. Stable and unstable phases of a diblock copolymer melt. *Physical Review Letters*, 72(16):2660–2663, 1994.
- [12] F. Drolet and G.H. Fredrickson. Combinatorial screening of complex block copolymer assembly with self-consistent field theory. *Physical Review Letters*, 83(21):4317–4320, 1999.
- [13] Z. Guo, G. Zhang, F. Qiu, H. Zhang, Y. Yang, and A.C. Shi. Discovering ordered phases of block copolymers: New results from a generic Fourier-space approach. *Physical Review Letters*, 101(2):28301, 2008.
- [14] K.Ø. Rasmussen and G. Kalosakas. Improved numerical algorithm for exploring block copolymer mesophases. *Journal of Polymer Science Part B: Polymer Physics*, 40(16):1777–1783, 2002.
- [15] E.W. Cochran, C.J. Garcia-Cervera, and G.H. Fredrickson. Stability of the gyroid phase in diblock copolymers at strong segregation. *Macromolecules*, 39(7):2449–2451, 2006.
- [16] R.B. Thompson, K.Ø. Rasmussen, and T. Lookman. Improved convergence in block copolymer self-consistent field theory by Anderson mixing. *The Journal of Chemical Physics*, 120:31, 2004.
- [17] H.D. Ceniceros and G.H. Fredrickson. Numerical solution of polymer self-consistent field theory. *Multiscale Modeling and Simulation*, 2:452–474, 2004.
- [18] P. Stasiaka and M.W. Matsen. Efficiency of pseudo-spectral algorithms with Anderson mixing for the SCFT of periodic block-copolymer phases. *The European Physical Journal E*, 34:110, 2011.
- [19] K. Jiang, Y. Huang, and P. Zhang. Spectral method for exploring patterns of diblock copolymers. *Journal of Computational Physics*, 229:7796–7805, 2010.
- [20] G.H. Fredrickson. *The equilibrium theory of inhomogeneous polymers*. Oxford University Press, USA, 2006.
- [21] L. Leibler. Theory of microphase separation in block copolymers. *Macromolecules*, 13(6):1602–1617, 1980.
- [22] D.A. Hajduk, P.E. Harper, S.M. Gruner, C.C. Honeker, G. Kim, E.L. Thomas, and L.J. Fetters. The gyroid: a new equilibrium morphology in weakly segregated diblock copolymers. *Macromolecules*, 27(15):4063–4075, 1994.
- [23] I.Y. Erukhimovich. Weak segregation theory and non-conventional morphologies in the ternary ABC triblock copolymers. *The European Physical Journal E*, 18(4):383–406, 2005.
- [24] A. Ranjan and D.C. Morse. Landau theory of the orthorhombic Fddd phase. *Physical Review E*, 74(1):11803, 2006.
- [25] N.F.M. Henry and K. Lonsdale. *International tables for X-ray crystallography*. Kynoch Press, 1952.
- [26] G.H. Fredrickson and E. Helfand. Fluctuation effects in the theory of microphase separation in block copolymers. *The Journal of Chemical Physics*, 87:697, 1987.
- [27] E. Abreu, J. Douglas, F. Furtado and F. Pereira. Operator splitting for three-Phase flow in heterogeneous porous media. *Communications in Computational Physics*, 6(1):72–84, 2009.